Presented at the Toulouse International
Conference on High Voltage Electron
Microscopy, Toulouse, France,
September 1 - 4, 1975

LBL-4114
CONF-750982--3

HIGH VOLTAGE ELECTRON MICROSCOPE STUDIES OF CERAMIC FERRITES

Gareth Thomas

MASTER

September 1975

Prepared for the U. S. Energy Research and
Development Administration under Contract W-7405-ENG-48

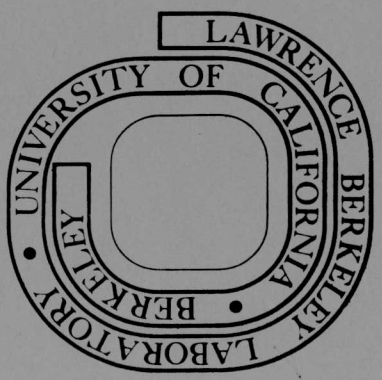

RECEIVED BY TIC MAR 10 1976

LBL-4114

DISTRIBUTION OF THIS DOCUMENT IS UNLIMITED

DISCLAIMER

This report was prepared as an account of work sponsored by an agency of the United States Government. Neither the United States Government nor any agency thereof, nor any of their employees, makes any warranty, express or implied, or assumes any legal liability or responsibility for the accuracy, completeness, or usefulness of any information, apparatus, product, or process disclosed, or represents that its use would not infringe privately owned rights. Reference herein to any specific commercial product, process, or service by trade name, trademark, manufacturer, or otherwise does not necessarily constitute or imply its endorsement, recommendation, or favoring by the United States Government or any agency thereof. The views and opinions of authors expressed herein do not necessarily state or reflect those of the United States Government or any agency thereof.

DISCLAIMER

Portions of this document may be illegible in electronic image products. Images are produced from the best available original document.

NOTICE
This report was prepared as an account of work sponsored by the United States Government. Neither the United States nor the United States Energy Research and Development Administration, nor any of their employees, nor any of their contractors, subcontractors, or their employees, makes any warranty, express or implied, or assumes any legal liability or responsibility for the accuracy, completeness or usefulness of any information, apparatus, product or process disclosed, or represents that its use would not infringe privately owned rights.

HIGH VOLTAGE ELECTRON MICROSCOPE STUDIES OF CERAMIC FERRITES

Gareth Thomas *

Department of Materials Science and Engineering, College of Engineering, and Inorganic Materials Research Division, Lawrence Berkeley Laboratory, University of California, Berkeley, California 94720.

INTRODUCTION

It is now appreciated that the principal advantages of HVEM are 1) increased penetration 2) increased resolution 3) decrease in inelastic scattering (and thus bond-breaking damage) 4) special effects due to multiple beam interactions e.g. critical voltage, increased resolution of lattice defects using high order bright field imaging etc. and some examples of applications have been reviewed recently[1]. The knock-on damage effect can be advantageous or not; its effect clearly limits the maximum voltage that can be used if knock-on damage is undesirable. As a result of these advantages we are now able to study difficult to thin and beam sensitive materials e.g. ceramics and polymers. In this paper emphasis will be placed on recent studies of defects and phase transformations in ceramic ferrites.

We are interested in the ferrites because of their great commercial importance due to their unique magnetic and electronic properties. Both hard and soft ferrites are extensively used in manufacturing microwave device-components, computer cores and permanent magnets. Ferrimagnetic oxides with spinel structure form an important class of the ferrites. Conventionally, grain size and porosity have been used for controlling properties in these materials, but it is very likely that heat treatments producing appropriate microstructures could lead to highly desirable properties. Thus the HVEM is essential to obtain basic structural information if progress is to be made in ceramics comparable to that in physical metallurgy. In a continuing program on microstructural characterisation in these materials, studies of phase transformations such as ordering and precipitation reactions as well as analysis of defects have been carried out with particular emphasis to lithium ferrite ($LiFe_5O_8$) spinel. The results are given in the following.

I. Phase Transition Studies

A. Dynamic Studies of Order-Disorder in $LiFe_5O_8$ (O. Van der Biest) (1MeV)

Lithium ferrite ($LiFe_5O_8$) is a ferrimagnetic compound with some interesting technological properties[2]. Many of the properties of interest are influenced by the degree of order in the compound. The most important of these is the DC electrical resistivity which changes by several orders of magnitude upon ordering. Other properties such as the ferrimagnetic resonance line-width, the magneto-crystalline anisotropy constants and, for polycrystalline samples, the squareness of the hysteresis loop are all influenced to a lesser degree by the state of order.

In the disordered state the compound has the inverse spinel structure with a random mixture of $1Li^+$ and $3Fe^{3+}$ on the octahedral sites (spacegroup Fd3m). Below 750°C the lithium ions and iron ions on the octahedral sites order and the space group symmetry is lowered to $P4_132$ ($P4_332$). The resulting domain structure has been described in detail by Van der Biest and Thomas[3].

The kinetics of the ordering reactions have been studied in single crystals "in situ" in the hot stage of a HVEM. Annealing in the normal atmosphere of the microscope leads to a reduction of the compound in a way similar to that found for $CoFe_2O_4$[4]. In order to control the stoichiometry of the compound during the ordering reaction, it is necessary to maintain an oxygen atmosphere around the specimen, hence the use of an "environmental" cell is necessary. In this study the environmental cell designed by Swann[5] for the Imperial College HVEM was used. An oxygen pressure of 40 Torr was found to be high enough to prevent rapid reduction of the compound and low enough to have sufficient penetration and contrast in the images. Radiation damage definitely played a role during the experiments. Prolonged focussing of the beam (>10 min) on one spot caused voids to nucleate and grow until holes were formed. It was also observed that the amount of damage was proportional to the time the specimen had spent above the ordering temperature. This suggests that the rate of damage is an order of magnitude larger in the disordered state for approxi-

*Invited Paper: International Conference on High Voltage Electron Microscopy, Toulouse, France, Sept. 1-4, 1975.

DISTRIBUTION OF THIS DOCUMENT IS UNLIMITED

mately the same temperature. The specimen was heated above Tc to about 770°C and then cooled as fast as the stage permits, to temperatures slightly below the ordering temperature (735°C - 745°C). The changes in microstructure were followed in dark field with a superlattice spot. Images were recorded with a low light level TV system on videotape with a speed of 25 frames/sec. Figure 1 shows a disordering sequence. It can be seen that disordering starts at the anti-phase boundaries, which are replaced by a layer of disordered material. The domains subsequently shrink and disappear if heating is slow or the contrast may fade uniformly before the domains can disappear by shrinking. Figure 2 shows an ordering sequence. Individual domains can be seen nucleating and growing, until they impinge and form antiphase domain boundaries.

The ordering reaction provides an example of the phase transformation with homogeneous nucleation and perfectly spherical growth. Studies of the nucleation rate as a function of undercooling indicate that the rate of nucleation follows the pattern predicted by the classical theory of homogeneous nucleation. Within a small range of undercooling, the nucleation rate increases by orders of magnitude. The growth rate of the domain is perfectly constant, until the domains touch one another. The growth rate as a function of undercooling was found to exhibit a maximum. This agrees with the theory of thermally-activated growth, where atomic processes at the interface are rate controlling. The mobility of the boundaries which form when two domains touch was immeasurable on the time scale of the experiments.

We are indebted to Dr. P. R. Swann for the use of the 1 MeV microscope at Imperial College and Dr. E. P. Butler for help with these experiments. The National Science Foundation provided a grant for this work.

B. High Temperature Phase Transformation in $LiFe_5O_8$ (R. Mishra) (650 kV)

In addition to the order-disorder phase transition at about 750°C in $LiFe_5O_8$, at higher temperature there occurs a precipitation reaction. This transformation was studied at 1200°C in air and in vacuum (10^{-5} torr). Specimens for HVEM observation were prepared from the center of 15 mil thick heat-treated single crystal discs using the ion bombardment technique.

The microstructure for short annealing times consists of small octahedral precipitates dispersed in the spinel matrix as shown in Fig. 3a. The precipitate phase has been identified to be lithium ferrate ($LiFeO_2$) having a NaCl structure and lattice parameter 4.14Å (a_{spinel} = 8.33Å). Computation of interfacial energy and strain energy for these particles show that the most favourable shape would be an octahedron with {111} crystallographic planes as faces. In terms of the structure of the two phases, this amounts to the oxygen layers in the spinel and the precipitate being indistinguishable and the only difference is in the cation distribution in the interstices. For longer annealing times, these particles grow and become semicoherent, (Fig. 3b), when their average size exceeds 2500Å. The dislocations at the interfaces have Burgers vectors parallel to <110>. Measurement of the separation between the interfacial dislocations give their magnitude to be 1/2<110> for a lattice misfit of 0.6%. The $LiFeO_2$ phase has been observed to transform to a spinel phase for very long aging times. The available phase diagram on Li_2O - Fe_2O_3 system cannot explain this formation of $LiFeO_2$ from nearly stoichiometric $LiFe_5O_8$.

The formation of a glassy phase has been observed both in air and in vacuum. The glassy particles form very rapidly in vacuum-annealed specimens while they do not form in the air-annealed specimens until the $LiFeO_2$ phase has transformed back to spinel. Fig. 4a is the microstructure obtained after prolonged annealing in air, and Fig. 4b shows preferential growth of the glassy phase at the $LiFe_5O_8$-$LiFeO_2$ interface in vacuum. We believe that this phase is due to the presence of residual flux in the flux grown spinel single crystals.

II. Study of the Defects (650 kV)

A. The study of Stacking Faults in Nickel Ferrite (M. Kao)

The ferrimagnetic $NiFe_2O_4$, with an inverse spinel structure possess a high Curie temperature (580°C) along with low dielectric loss[2] and is one of the commercial ferrites used in high speed computer memory units. Electron microscopy observation of some sintered finegrain polycrystalline $NiFe_2O_4$ samples has shown cation faults in most grains. Due to the very small grain sizes of many commercial ferrites, contrast analysis becomes difficult and tedious. However, analysis of a threefold

junction shown in Figure 5 is possible using <131>, <220> and <151> sets of reflections in our 650 kV microscope due to our large angle double tilt stage. The results confirm that the faults are on {110} with 1/4<110> fault vectors normal to the fault planes. This fault configuration is similar to that reported for $LiFe_5O_8$[6]. It may be noted that faults in {001} planes, reported for the normal spinel $MgAl_2O_4$[9] have not been observed in any of these inverse spinels.

B. 1) Cation Faults in Lithium Ferrite: New Contrast Result (R. Mishra)

In flux grown $LiFe_5O_8$ single cyrstals as well as sintered nickel ferrite polycrystals cation faults with $\alpha = \pm\pi$ have been observed, and have been characterised as {110}1/4<110> growth faults[6]. Also, in our laboratory faults with $\alpha = \pm\pi$ have been observed in a sintered silicon carbide polycrystals. Special contrast effects occur for $\alpha = \pm 2\pi/3$ faulting in dark field images in $\pm g$ for $\pm 2g$ satisfied for systematic reflections and have already been described[7]. Similar imaging conditions can be used for rapid determination of the fault plane by identifying the top and bottom of the fault plane even when $\alpha = \pm\pi$. Figure 6a and 6b are D.F. pictures taken with g and -g, respectively, when 2g is excited. The computed fringe profiles for the two cases are shown in Figures 6c and 6d. While the contrast difference in g, 2g is not very pronounced, the fringes in -g, 2g condition show pronounced contrast corresponding to the bottom of the foil. The result has been confirmed by determing the actual fault plane from detailed contrast experiments.

2) Dissociated Dislocations and Stacking Fault Energy in $LiFe_5O_8$ (R. Mishra)

The multibeam dynamical interaction effect giving rise to increased resolution in B.F. images when a high order reflection in a systematic row is excited[7] has been used to resolve the partial dislocations in disordered lithium ferrite spinel. Figure 7 shows the B.F. Micrograph along with a microdensitometer trace and the computed image profile for the two partials with b = 1/4[011]. The dissociation can be represented as 1/2[011] = 1/4[011] + 1/4[011] on the $(01\bar{1})$ plane connected by a stacking fault 220Å wide in the cation sublattice. The splitting here corresponds to a stacking fault energy of about 75 ergs/cm^2. Computation for inverse spinel gives a value of 80 ergs/cm^2 for lithium spinel[8]. This is the first time a stacking fault energy has been measured for an inverse spinel.

I am pleased to acknowledge continued financial support from the U.S. Energy Research and Development Administration through the Inorganic Materials Research Division of the Lawrence Berkeley Laboratory. I am grateful to members of my ceramics group for providing me with the examples for this paper. Their names are indicated in the appropriate sections.

REFERENCES

1. Thomas, G., (1975) Physical Aspects of Electron Microscopy and Microbeam Analysis, Eds. B. M. Siegel and D. R. Beaman, 81.
2. Hellwege, K.-H. and Hellwege, A. M., (Eds.) (1970) Magnetic and Other Properties of Oxides and Related Compounds, Landolt-Bornstein Tables, III/4, Springer Verlag.
3. Van der Biest, O. and Thomas, G., (1975) Acta Cryst., A31, 70.
4. DeJonghe, L. C. and Thomas, G., (1971) Materials Science and Engineering, 8, 259.
5. Swann, P. R., (1972) Electron Microscopy and Structure of Materials, Eds. G. Thomas, R. Fulrath and R. Fisher, University of California Press, 878.
6. Van der Biest, O. and Thomas, G. (1974) Phys. Stat. Solidi, 24, 65.
7. Chen, L. J., and Thomas, G., (1974) Phys. Stat. Solidi, 25, 193.
8. Mishra, R. K., Ph.D. Thesis in Progress.
9. Lewis, M. H., (1966) Phil. Mag. 14, 1003.

Figure Captions

Fig. 1. Disordering sequence in situ at 1 MeV under 40 torr oxygen pressure. Disordering nucleates at APB's. Dark field image of 112 superlattice spot.

Fig. 2. Ordering sequence followed dynamically in situ at 1 MeV, as for Fig. 1. Darkfield images of the 112 superlattice spot.

Fig. 3. (a) Octahedral precipitates of $LiFeO_2$ in $LiFe_5O_8$, imaged near the (110) pole. (b) Growing $LiFeO_2$ precipitates with semicoherent interfaces.

Fig. 4. (a) Glassy particles dispersed in lithium spinel phase. (b) Preferential growth of glassy phase at $LiFeO_2$-$LiFe_5O_8$ interface. Note the elongated $LiFeO_2$ particle morphology parallel to $[2\bar{2}0]$.

Fig. 5. Cation faults in polycrystalline nickel ferrite ($NiFe_2O_4$). The threefold fault junction is inside a grain. (a) $g = 1\bar{3}1$ (b) $g = \bar{1}\bar{3}1$.

Fig. 6. D. F. image of cation faults in $LiFe_5O_8$, $s_{2g} = 0$, (a) image of g (b) image of -g (c) and (d) corresponding computed profiles (8 beam systematic $\langle 220 \rangle$).

Fig. 7. (a) Dissociated dislocations in $LiFe_5O_8$ imaged near (110) pole. (b) Microdensitometer trace at A (c) computed profile for 1/2[011]=1/4[011]+1/4[011].

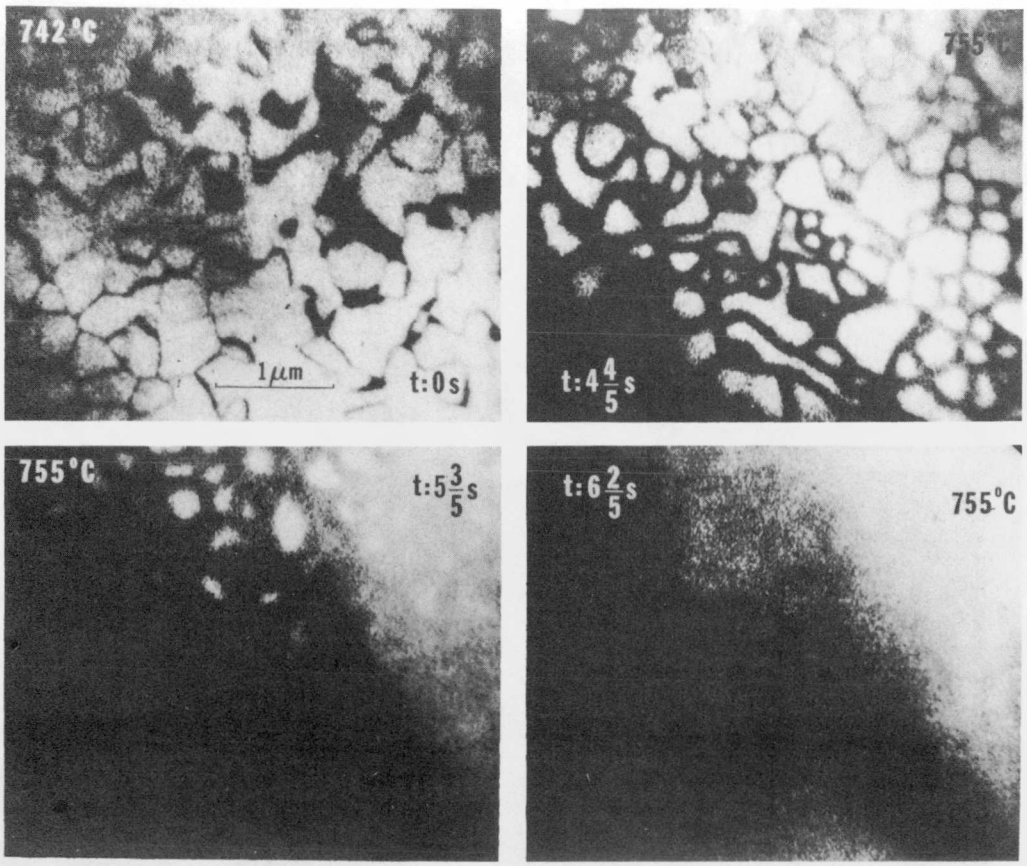

XBB 753-2230

Fig. 1

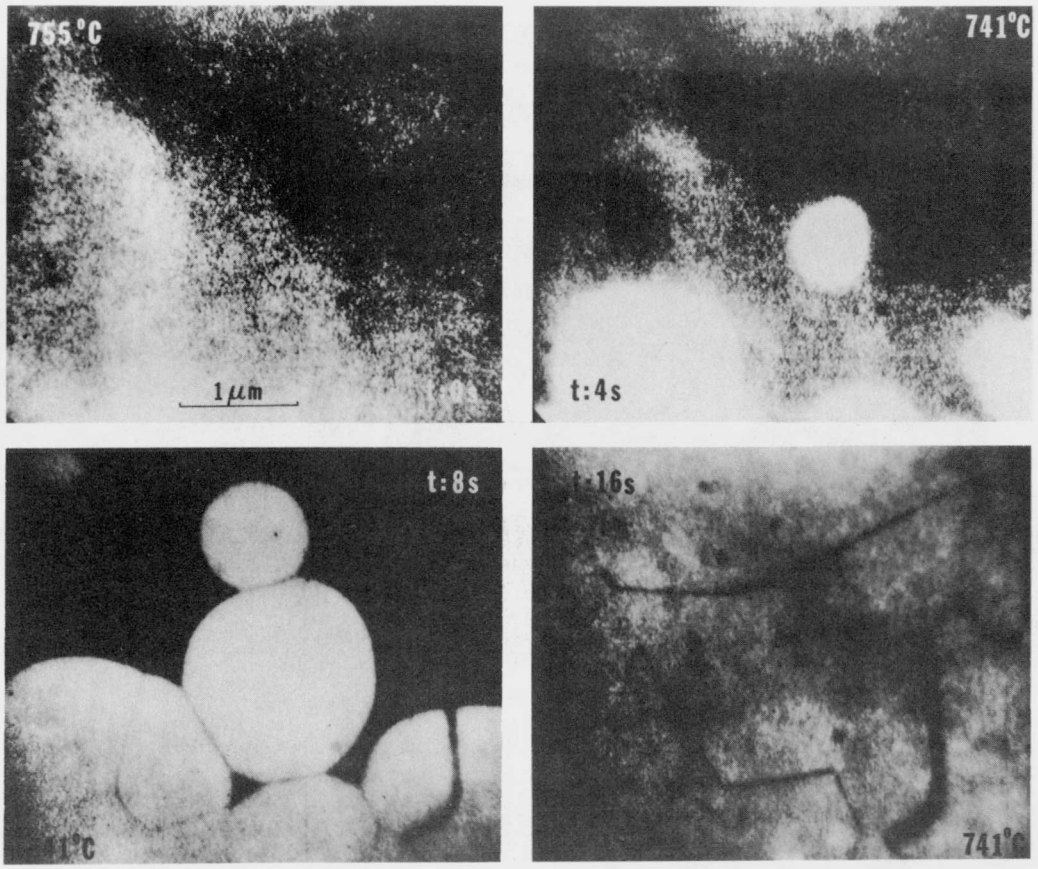

XBB 753-2231

Fig. 2

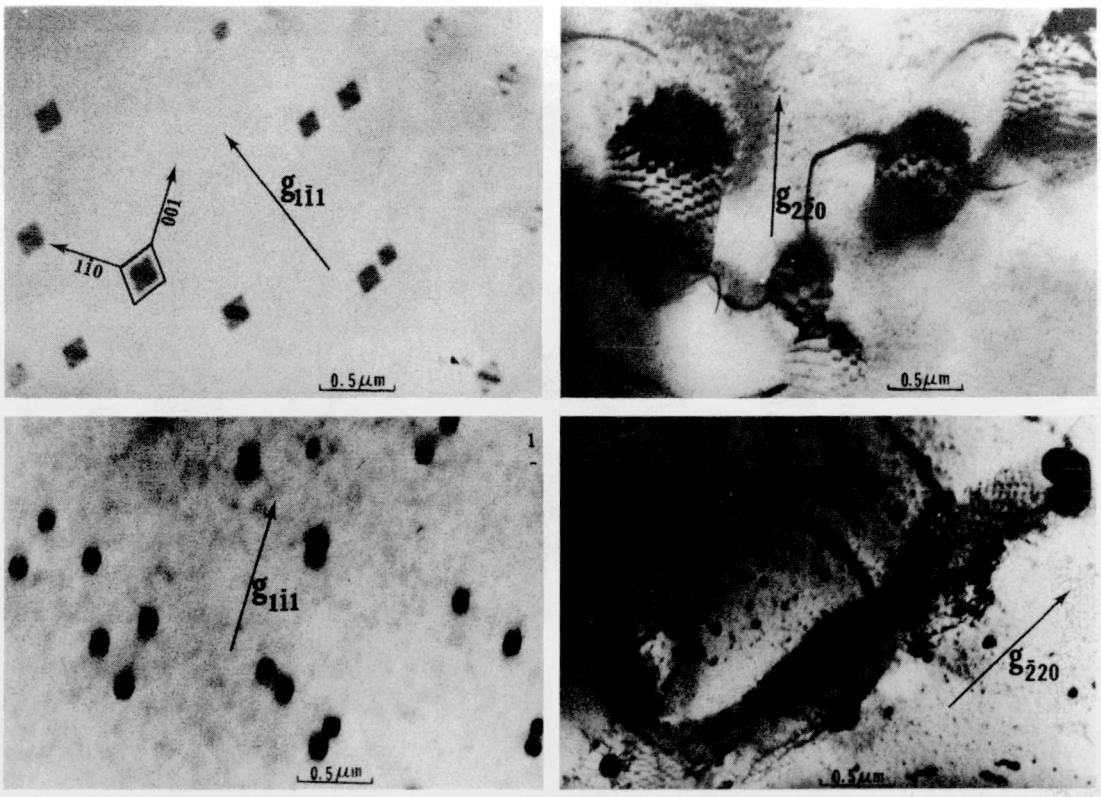

XBB 758-5807

Fig. 3 Top

Fig. 4 Bottom

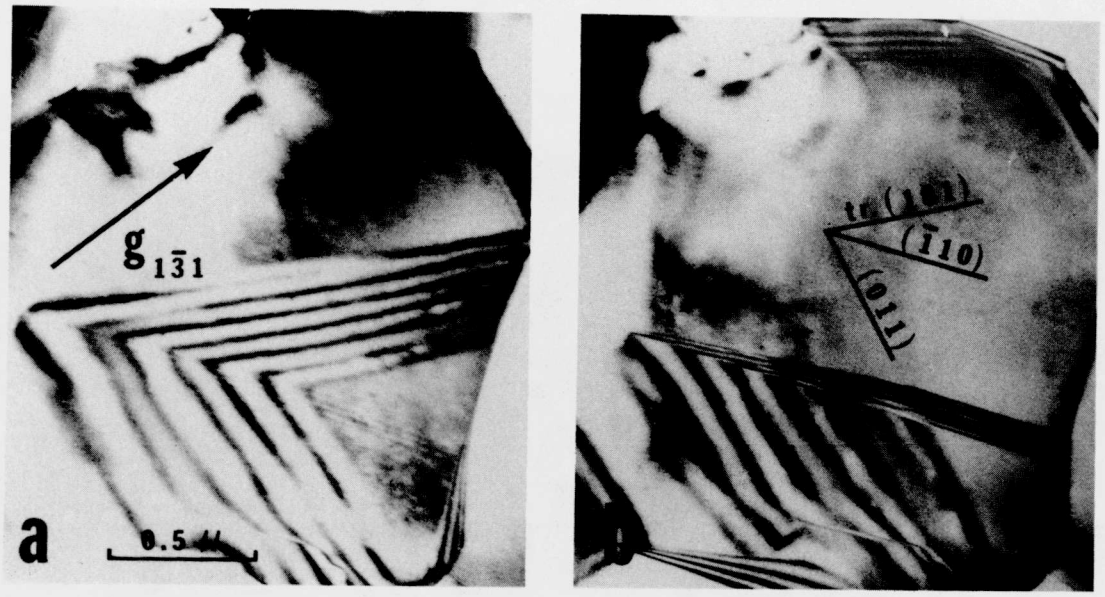

XBB 7511-8375

Fig. 5

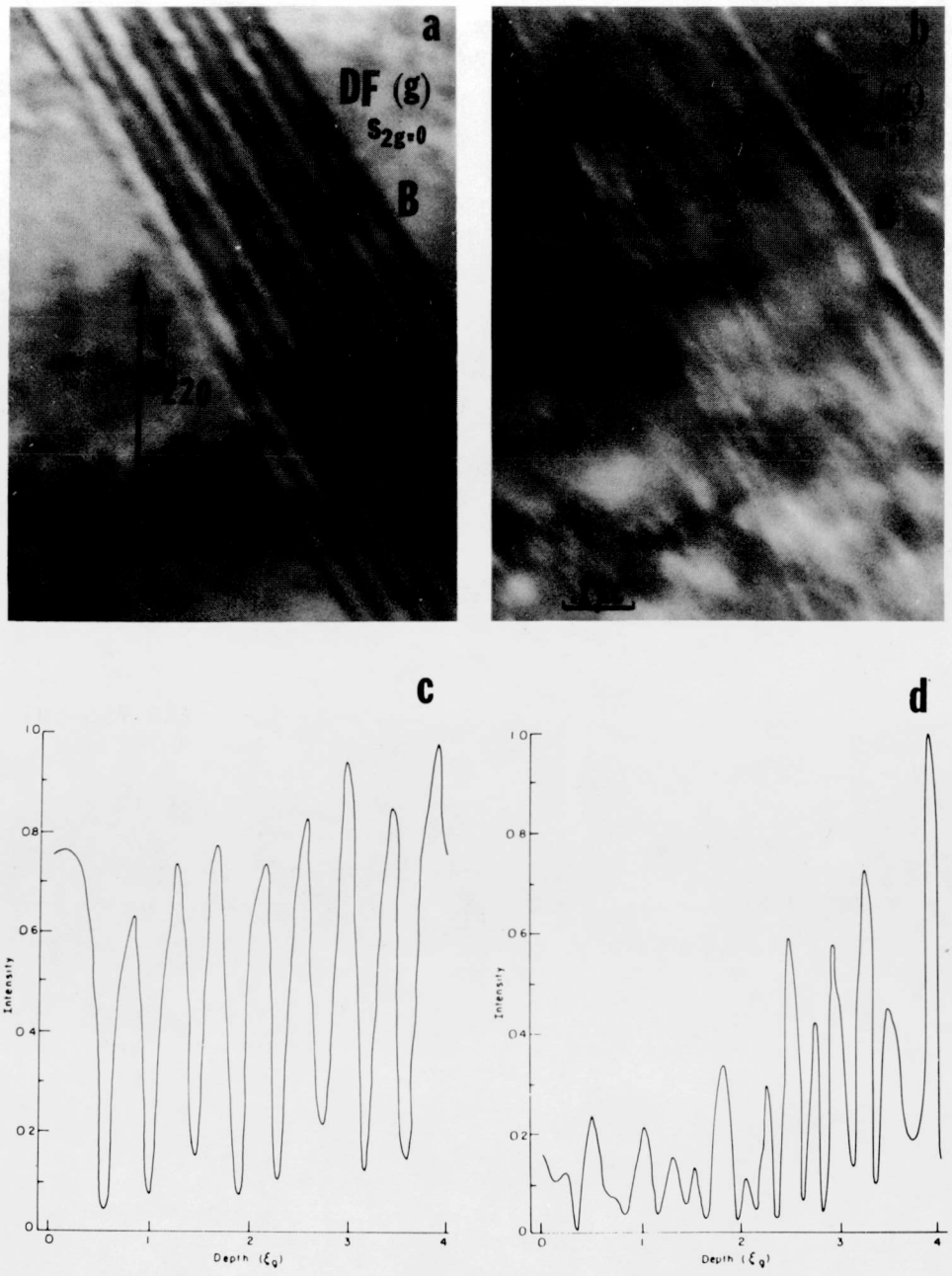

XBB 758-5878

Fig. 6

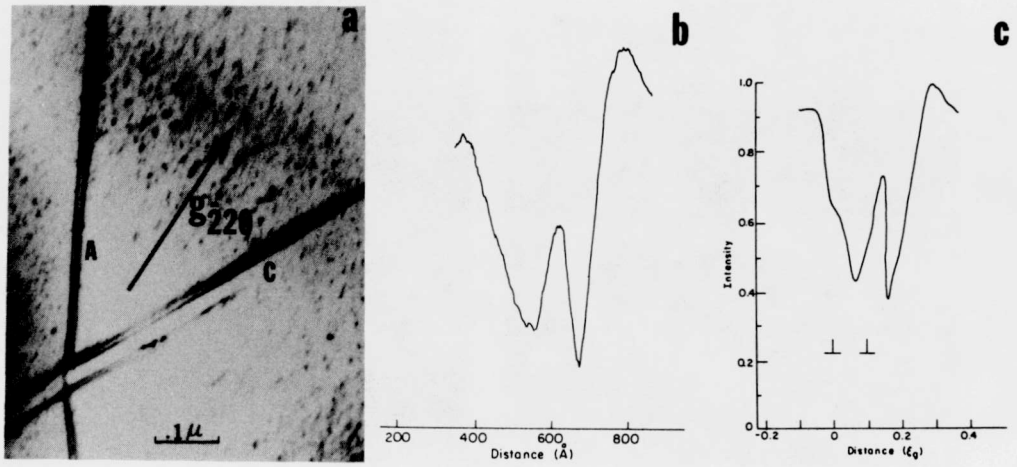

XBB 758-5877

Fig. 7

LEGAL NOTICE

This report was prepared as an account of work sponsored by the United States Government. Neither the United States nor the United States Energy Research and Development Administration, nor any of their employees, nor any of their contractors, subcontractors, or their employees, makes any warranty, express or implied, or assumes any legal liability or responsibility for the accuracy, completeness or usefulness of any information, apparatus, product or process disclosed, or represents that its use would not infringe privately owned rights.

TECHNICAL INFORMATION DIVISION
LAWRENCE BERKELEY LABORATORY
UNIVERSITY OF CALIFORNIA
BERKELEY, CALIFORNIA 94720